

Multipartite entangled microwave and micromechanical squeezed Schrödinger cats: a phase transition-based protocol

A. A. Gangat,¹ I. P. McCulloch,¹ and G. J. Milburn¹

¹*Department of Physics, School of Mathematics and Physics,
The University of Queensland, St Lucia, QLD 4072, Australia*

Abstract

Here we present a novel scheme to generate, on demand, large amplitude multipartite squeezed entangled coherent states (ECSs) [17, 18] via a (pseudo-)quantum phase transition [19] of the attractive Bose-Hubbard model (ABH). We show that current technology can be used to implement the scheme in a coupled array of superconducting non-linear microwave resonators tunably coupled to an array of uncoupled micromechanical oscillators. The result is an array of squeezed Schrödinger cats that are non-locally entangled across a large number of microwave and/or micromechanical local or normal modes.

Optomechanical and nanoelectromechanical [1, 2] systems currently offer a path to engineering coherent quantum systems capable of supporting macroscopic quantum states, such as Fock states [3], cat states [4] and entangled states of distinct mechanical elements [5]. This would enable new quantum metrological devices [6–8], integration of mechanical oscillators into classical [9] and quantum information processing components [10–12], and possibly tests of quantum gravity effects [13] and gravitational and non-gravitational collapse theories [14–16].

Observing the quantum behaviour of macroscopic mechanical objects has received serious consideration in the literature since near the beginning of the century [20–27], and in 2010 O’Connell et al. [3] demonstrated for the first time a non-classical state of a macroscopic mechanical object by placing the dilational mode of a micromechanical resonator in a quantum superposition of the ground state and the first excited state. To date, however, mechanical entanglement, mechanical squeezing, and superpositions of ”macroscopically distinct” [28] mechanical states (Schrödinger cats) remain unobserved. Non-local mechanical entanglement, first considered by Mancini et al. [5], is of fundamental interest as it would further elucidate the nature of the quantum-classical boundary and may provide the opportunity for teleporting the quantum state of the centre of mass of a macroscopic object [29]. From an applied perspective, the force-sensing capability of mechanical oscillators may be enhanced by entanglement [30], and the expected long coherence times of mechanical oscillators at low temperatures may make them useful for quantum information processing (QIP). Squeezed mechanical states [22], where the quantum noise in one quadrature of the mechanical oscillator is reduced below the standard quantum limit, in addition to being of interest in exploring the quantum-classical boundary can also be useful for metrology [31]. Finally, mechanical Schrödinger cats are relevant to tests of various models of environmentally induced decoherence [32] in mechanical resonators [33, 34] and tests of gravitational and non-gravitational wavefunction collapse theories (see [15] for a review or [16] for a summary).

ECSs (see [18] for a review) are able to combine Schrödinger cats and non-local entanglement in a single multipartite state such that, ”The individual coherent states retain the desirable quasiclassical properties of coherent states but nonlocal features arise due to the entanglement” [17]. It is therefore highly desirable to create ECSs of mechanical resonators with squeezed coherent states as this would simultaneously encapsulate mechanical entanglement, squeezing, and Schrödinger cats. Bose and Agarwal proposed a scheme [35] to create

an ECS with two nanomechanical resonators (NRs) coupled to a cooper pair box (CPB), and Tian and Zoller [36] considered ECS creation in the situation of two NRs coupled to a trapped ion. However, both schemes are not readily scalable to larger numbers of resonators, do not involve squeezed states, and remain experimentally underdeveloped.

In the photonic domain there has been much theoretical interest in ECS generation and use at optical frequencies [18], and the first experimental demonstration of ECS generation was published in 2009 by A. Ourjoumtsev et al. [38] for the case of two distant optical modes. Generating ECSs in superconducting microwave circuits, however, has received little attention. Superconducting circuits are an important platform for QIP and scale much more easily to large numbers of cavities than do optical setups. This is particularly significant for W-ECSs (ECSs of the form $|\alpha, 0, 0, \dots, 0\rangle + |0, \alpha, 0, \dots, 0\rangle + \dots + |0, 0, 0, \dots, \alpha\rangle$), as the bipartite and global entanglement decay under dephasing and the global entanglement decay under amplitude damping have been shown to be independent of the number of qubits for the discrete variable W states [39], which are of the same general form as W-ECSs. To date, there have been no proposals to our knowledge to generate W-ECSs in microwave circuits.

Here we present the first scheme to deterministically prepare large amplitude ($|\alpha|^2 \gg 1$) squeezed W-ECSs in an array of coupled superconducting microwave coplanar waveguides (CPWs) and to subsequently transfer them to an array of uncoupled micromechanical oscillators. We employ a new paradigm, dynamical ECS generation via a (pseudo-)quantum phase transition [19] of a many-body Hamiltonian, which naturally accommodates a large number of oscillators and is particularly well-suited to the platform of superconducting circuits [40]. Our scheme is also the first to be able to distribute ECSs amongst the fundamental normal modes of distinct oscillator arrays [41], thereby producing non-locally superposed microwave/micromechanical coherent state superfluids. We design our scheme around existing technology, as we describe below, and estimate that parameters within the reach of present-day devices can yield a purely mechanical version of the squeezed W-ECS with a multipartite superposition coherence of greater than fifty percent for an initial coherent state of amplitude $|\alpha|^2 \approx 20$. We also perform a numerical verification of our scheme in the absence of dissipation for the case of two microwave cavities. Further to the squeezed W-ECS of the form $\frac{1}{\sqrt{M}} \sum_{j=1}^M |\alpha_{sq}\rangle_j (\Pi_{r \neq j} \otimes |0\rangle_r)$, where $|\alpha_{sq}\rangle$ denotes a quadrature squeezed coherent state, our scheme can also generate the squeezed W-type entangled Schrödinger cat state (squeezed W-ESCS): $\frac{1}{\sqrt{M}} \sum_{j=1}^M \frac{1}{\sqrt{2}} (e^{-i\pi/4} |i\alpha_{sq}\rangle_j + e^{i\pi/4} |-i\alpha_{sq}\rangle_j) (\Pi_{r \neq j} \otimes |0\rangle_r)$, as well as the

squeezed GHZ-ECS: $\frac{1}{\sqrt{2}}(e^{-i\pi/4}|i\frac{\alpha_{sq}}{M}\rangle_1|i\frac{\alpha_{sq}}{M}\rangle_2\dots|i\frac{\alpha_{sq}}{M}\rangle_M + e^{i\pi/4}|-i\frac{\alpha_{sq}}{M}\rangle_1|-i\frac{\alpha_{sq}}{M}\rangle_2\dots|-i\frac{\alpha_{sq}}{M}\rangle_M)$.

The W-ECS, W-ESCS, and GHZ-ECS, in addition to being either purely microwave or purely micromechanical, may be distributed amongst a combination of microwave and micromechanical oscillators.

I. SYSTEM AND MODEL

We consider a one-dimensional chain of sites with periodic boundary conditions (Fig. 1). Each site consists of a superconducting microwave frequency CPW resonator, and the microwave LC electromechanical system demonstrated by Teufel et al. in [43, 44]. A transmon qubit SQUID is embedded in the CPW resonator, as in the case theoretically analyzed in [45], which induces a Kerr nonlinearity in the fundamental microwave mode c of the CPW: $H_c = \hbar\omega_c c^\dagger c - \hbar\frac{\chi}{2}c^\dagger c(c^\dagger c - 1)$; ω_c and χ , respectively the frequency and Kerr constant of the mode, are dependent on the flux through the SQUID loop, with ω_c achieving a minimum for the flux value that maximizes χ_c and vice versa. The electromechanical system can achieve ground state cooling of the mechanical mode b and the quantum-coherent strong-coupling interaction Hamiltonian $H_{int} = -\hbar g(a^\dagger b + ab^\dagger)$ when driven at the red mechanical sideband of the fundamental LC microwave mode a , with g as the interaction strength. State swapping between modes a and b was recently demonstrated [46]. The fundamental CPW mode c is coupled to the LC mode a via the tunable coupler demonstrated in [47, 48]. The chain is formed by linking the fundamental modes c_j of nearest neighbour CPWs, where j is the site index, also with the tunable coupler.

All of the relevant dynamical time scales for our proposed system are much shorter than the dissipation time scales of the relevant degrees of freedom. The microwave mode a of the electromechanical system has frequency $\omega_a/2\pi \simeq 7.5$ GHz [43, 44], and referring to [45] we find that it is reasonable to choose $\omega_c/2\pi \simeq 4.5 - 7.5$ GHz and $\chi_c/2\pi \simeq 400 - 0$ MHz for the flux-tunable frequency and concomitant Kerr constant ranges of the CPW mode c so that it is on resonance with mode a when $\chi = 0$. ω_c and χ may be tuned over their respective ranges in ~ 5 ns [45]. The mechanical mode b has frequency $\omega_b \simeq 2\pi \times 10.6$ MHz [43, 44]. The highest coupling rate g/π seen between modes a and b is ~ 5 MHz [49], and the coupling rate $\kappa'/2\pi$ between modes a_j and c_j for the device demonstrated in [47] is tunable over the range $0.1 \leq \kappa'/2\pi \leq 50$ MHz on a timescale of ~ 2 ns. Reference [47] also predicts that with

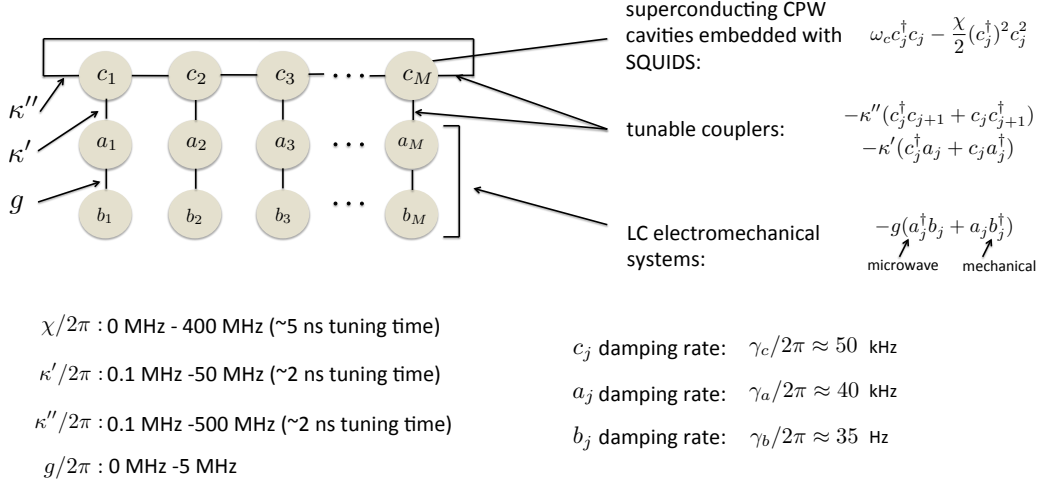


FIG. 1: Proposed system and parameters. Beige circles denote microwave CPW (c_j), microwave lumped LC (a_j), and micromechanical (b_j) oscillator modes. Solid black lines denote tunable inter-mode coupling. The CPWs are embedded with transmon SQUIDS to give a negative Kerr nonlinearity to the c_j modes. Each CPW is tunably coupled to an electromechanical system, represented by modes a_j and b_j , of the type of Teufel et al. [43, 44].

minor modifications to the device, the range $0.1 \leq \kappa''/2\pi \leq 500$ MHz should be possible for the coupling rate $\kappa''/2\pi$ between modes c_j and $c_{j\pm 1}$. The intrinsic amplitude damping rate for the fundamental microwave mode of the system of Teufel et al. is $\gamma_a \sim 2\pi \times 40$ kHz, while that of the fundamental mechanical mode is $\gamma_m \sim 2\pi \times 35$ Hz [46]. The CPW T_1 time in the NOON state experiment of Wang et al. [50] is $\sim 3 \mu\text{s}$ ($\gamma_c \approx 2\pi \times 53$ kHz), and we neglect the dephasing time as is always done for superconducting CPWs. The transmon has been experimentally shown to have a $T_1 > 1.5 \mu\text{s}$ and a minimum T_ϕ of $\geq 35 \mu\text{s}$ [51]. The minimum value of T_ϕ occurs at the flux sweet spot, but considering an asymmetric SQUID as in [45] allows for $T_\phi \gtrsim \text{ms}$ at the flux values where χ is minimum and maximum [52].

The model Hamiltonian for such a system, when the modes a_j are all driven with equal and sufficient strength at frequency ω_D near their red mechanical sidebands in the "resolved sideband" limit [2], can be expressed after appropriate transformations and approximations

as

$$\begin{aligned} \frac{H}{\hbar} = & \sum_{j=1}^M \delta_j a_j^\dagger a_j + (\delta_j - \Delta_j) c_j^\dagger c_j - \frac{\chi_j}{2} c_j^\dagger c_j (c_j^\dagger c_j - 1) \\ & - \kappa' (c_j^\dagger a_j + c_j a_j^\dagger) - \kappa'' (c_j^\dagger c_{j+1} + c_j c_{j+1}^\dagger) - g (a_j^\dagger b_j + a_j b_j^\dagger), \end{aligned} \quad (1)$$

where j is the site index, $c_{M+1} = c_1$ (periodic boundary conditions), $\delta_j = \omega_{a,j} - \omega_{b,j} - \omega_{D,j}$ is the detuning of the drives from the red mechanical sidebands, $\Delta_j = \omega_{a,j} - \omega_{c,j}$, $g = g_0 \sqrt{n_D}$, g_0 is the bare cavity optomechanical coupling, and n_D is the number of drive photons in the resonators of the modes a_j . The Hamiltonian preserves the total number of quanta in the system. Because of this and the fact that the dissipation time scales are much longer than the relevant dynamical time scales of the unitary evolution, we may consider the qualitative physics of the system in an isolated and number-conserving picture.

With uniform parameters ($\delta_j = \delta$, $\Delta_j = \Delta$, $\chi_j = \chi$, $\kappa'_j = \kappa''$), Eq. (1) is essentially the Hamiltonian for the one dimensional ABH with two additional degrees of freedom (a_j and b_j) linked to each lattice site. For $\kappa' \ll \kappa''$, these additional degrees of freedom are effectively decoupled from the lattice, and we may make a unitary transformation to recover the ABH that is theoretically studied in Refs. [53–62]:

$$\frac{H}{\hbar} = \sum_{j=1}^M -\frac{\chi}{2} c_j^\dagger c_j (c_j^\dagger c_j - 1) - \kappa'' (c_j^\dagger c_{j+1} + c_j c_{j+1}^\dagger), \quad (2)$$

In this way our proposed system is similar to that of [63] and provides a more robust alternative platform to BECs in optical lattices [53, 54], coupled atom-cavity systems [64], and trapped ions [58] for the experimental realization of the ABH. We also note that the combination of quartic and quadratic terms in Eq. (2), given sufficient time-dependent control over the χ_j and κ_j and supplemented by coherent displacements of the fields, should enable one to sue this system as a universal Bosonic simulator based on a result of Braunstein and Lloyd [65]. In the appendix we demonstrate this for the case of bipartite W-ECS creation.

In the ABH the ground state changes qualitatively as a function of the parameter $\tau = \frac{\kappa''}{\chi(N-1)}$, where N is the total number of quanta and we assume $N > 1$. Any particular realization of the ABH can be characterized by the constants τ_1 and τ_2 ($\tau_2 \geq \tau_1$) such that for $\tau > \tau_2$ the ground state is a superfluid, for $\tau_1 > \tau$ the ground state is a Schrödinger cat-like state, and the intermediate regime $\tau_2 > \tau > \tau_1$ is transitional in nature [54]. $\tau_1 \approx 0.25$

is largely independent of lattice size [54, 56], while $\tau_2 \approx [2M \sin^2(\pi/M)]^{-1}$ for $M > 5$ and $0.25 < \tau_2 \lesssim 0.3$ for $3 \leq M \leq 5$ [55]. $\tau_2 = \tau_1$ for $M = 2$ [56]. In this paper we are concerned with accessing the Schrödinger cat regime ($\tau < \tau_1$), where, for decreasing values of τ , the ground state approaches the W-state $|\Psi_N\rangle = \frac{1}{\sqrt{M}} \sum_{j=1}^M |N\rangle_j (\Pi_{r \neq j} \otimes |0\rangle_r)$, the on-site number fluctuations ($\sigma_j^2 = \langle c_j^\dagger c_j^\dagger c_j c_j \rangle - \langle c_j^\dagger c_j \rangle^2$) approach $N^2 \sqrt{M-1}/M$, and the single particle correlation between sites ($C_1 = \langle c_j^\dagger c_{j+1} \rangle$) approaches 0 [53, 54].

In [64] Brandao et al. suggested using an atom-cavity realization of the ABH to create a polaritonic (photon-atom hybrid) W-state in multiple optical cavities via adiabatic transition from the superfluid regime to the Schrödinger cat regime by tuning χ . This is possible also for the microwave quanta in our proposed system as the experimental parameter space that we specified above allows a minimum τ value of $0.00025/(N-1)$. However, by extension, a number distribution in the form of a coherent state $|\alpha\rangle = e^{-|\alpha|^2/2} \sum_{n=0}^{\infty} \frac{\alpha^n}{\sqrt{n!}} |n\rangle$ (with amplitude α large enough such that $|\langle 1|\alpha\rangle|^2 \lesssim 0.01$) can become a site-localized superposition of generalized coherent states: $|\Psi_{\alpha_{gen}}\rangle = \frac{1}{\sqrt{M}} \sum_{j=1}^M |\alpha_{gen}\rangle_j (\Pi_{r \neq j} \otimes |0\rangle_r) = \frac{1}{\sqrt{M}} \sum_{j=1}^M e^{-|\alpha|^2/2} \sum_{n=0}^{\infty} e^{i\phi_n} \frac{\alpha^n}{\sqrt{n!}} |n\rangle_j (\Pi_{r \neq j} \otimes |0\rangle_r)$; the linearity of quantum mechanics allows each number state component $|n\rangle$ of the coherent state $|\alpha\rangle$ to become a W-state $|\Psi_{N=n}\rangle$ by tuning χ , but an additional number-dependent phase factor $e^{i\phi_n}$ appears for each number state component due to the number-dependent frequency induced by the Kerr medium. For a coherent state of amplitude α localized on a single site, we have the exact relation $\phi_n = n \int \frac{\chi(t)}{2} dt$. For $M > 1$, although the coherent state in the lattice will start in the superfluid regime, if the majority of the number distribution becomes site-localized (i.e. $\tau = \frac{\kappa''}{\chi(n-1)} < 0.25$ for all n in the distribution within one standard deviation of $\langle n \rangle$) in a sufficiently short time, we may approximate $\phi_n \approx n \int \frac{\chi(t)}{2} dt$. Then, if $\frac{1}{2\pi} \int \chi(t) dt$ is an integer, the site-localized superposition approximately becomes the W-ECS: $|\Psi_{W-ECS}\rangle = \frac{1}{\sqrt{M}} \sum_{j=1}^M |\alpha\rangle_j (\Pi_{r \neq j} \otimes |0\rangle_r)$, and if $\frac{1}{\pi} \int \chi(t) dt$ is an odd integer, the site-localized superposition approximately becomes the W-ESCS: $|\Psi_{W-ESCS}\rangle = \frac{1}{\sqrt{M}} \sum_{j=1}^M \frac{1}{\sqrt{2}} (e^{-i\pi/4} |i\alpha\rangle_j + e^{i\pi/4} |-i\alpha\rangle_j) (\Pi_{r \neq j} \otimes |0\rangle_r)$ [66].

But the exact state of the system near the select values of $\int \chi(t) dt$ can actually be a squeezed W-ECS/W-ESCS. This can be seen as follows: In the superfluid regime the state of the system may be approximated as $|\frac{\alpha}{M}, \frac{\alpha}{M}, \dots, \frac{\alpha}{M}\rangle$, and the state evolution at each site as χ is tuned is approximately that of a coherent state in a Kerr medium with a time-increasing χ . The phase shearing of the state at each site before entering the Schrödinger cat regime

is therefore roughly $\frac{|\alpha|}{M} \int_0^{T^*} \chi(t) dt$, where T^* is the time taken to enter the Schrödinger cat regime. If this phase shearing is small (it can be shown that it is inversely proportional to $M|\alpha|$ since T^* itself is inversely proportional to $|\alpha|^2$), the coherent state $|\alpha/M\rangle$ at each site before the Schrödinger cat regime ($\tau < 0.25$) is entered becomes a quadrature squeezed coherent state (such quadrature squeezing at short times of a coherent state in a Kerr medium was demonstrated in the recent experiment of G. Kirchmair et al. [67] for the case of fixed χ). In this case the state of the system is a squeezed W-ECS immediately after the Schrödinger cat regime is entered at $t = T^*$ and for all later times $t = T$ when $\frac{1}{2\pi} \int_{T^*}^T \chi(t) dt$ is an integer. We demonstrate this numerically in section III. Further, when $\frac{1}{\pi} \int_{T^*}^T \chi(t) dt$ is an odd integer the result is a squeezed W-ESCS.

A more generalized form of the site-localized states $|\Psi_{\alpha_{gen}}\rangle$ is $|\Psi_{\alpha_{gen}}^{(block)}\rangle = \frac{1}{\sqrt{R}} \sum_{l=1}^R |\alpha_{gen}\rangle_l (\Pi_{r \neq j} \otimes |0\rangle_r)$, where the lattice is divided into a total of R adjacent blocks with an arbitrary number of sites in each (see Fig. (2) for an example), l and r are block indices, and $|\alpha_{gen}\rangle_l$ designates a generalized coherent state of amplitude α occupying the lowest energy normal mode of lattice block l : $|\alpha_{gen}\rangle_l = e^{-|\alpha|^2/2} \sum_{n=0}^{\infty} e^{i\phi_n} \frac{\alpha^n}{n!} (a_{l,k=0}^\dagger)^n |0\rangle_l$ ($a_{l,k=0}^\dagger$ is the creation operator for the lowest energy normal mode of block l). This cat state generalizes the W-ECSs studied in [68–71], which consist of coherent states confined to single local modes but entangled between multiple local modes, to W-ECS where any component of the superposition may be distributed over multiple spatially adjacent local modes. Such states may be thought of as non-local superpositions of superfluids. We next discuss the experimental protocol of how to prepare $|\Psi_{\alpha_{gen}}^{(block)}\rangle$ in our system and convert it into a purely mechanical state.

II. PREPARATION PROTOCOL

The experimental protocol for preparing $|\Psi_{\alpha_{gen}}^{(block)}\rangle$ in the c_j modes is illustrated in Fig. (2) for the case of $M = 3$ and $R = 2$. The couplings κ_j'' that cross block boundaries are specially designated as κ''' . At the beginning of the protocol, $\chi_j = 0$, and the microwave modes a_j and c_j are all in their ground states at cryogenic temperatures and are uncoupled by setting $\kappa' = 0.1$ MHz. After setting $\kappa_j'' = \kappa_{max}'' = 500$ MHz, a coherent drive is applied to the lowest energy normal mode of the c_j lattice to create a coherent state of amplitude α , after which the drive is turned off. This results in a product coherent state of the local

modes: $|\frac{\alpha}{M}\rangle_1|\frac{\alpha}{M}\rangle_2\ldots|\frac{\alpha}{M}\rangle_M$. The $n = 1$ component of the normal mode coherent state will not site-localize as τ is increased, so we require α sufficiently large such that $P_1 = |\langle 1|\alpha\rangle|^2$ is very small.

The first step of the protocol adiabatically transforms the multimode coherent state of the c_j modes into $|\Psi_{\alpha_{gen}}\rangle$ by increasing χ . From the discussion in section I., we know that for increasing values of χ/κ'' the ground state with $N = n$ is transformed at the critical point $\chi/\kappa'' \approx 4/(n-1)$ to a Schrödinger cat-like state. Considering the largest value of χ as $\chi_{max}/2\pi = 400$ MHz, the bound on the smallest non-negligible Fock state component $|n_{min}\rangle$ of the coherent state must be $n_{min} \geq \frac{4\kappa''_{max}}{\chi_{max}} + 1 = 6$. Setting $\sum_{n=0}^5 |\langle n|\alpha\rangle|^2 \leq 0.01$, we find that $|\alpha|^2 \geq 14$ is sufficient to be able to neglect number state components with $n < 6$.

Tuning τ through the transition (by changing χ) to achieve $|\Psi_{\alpha_{gen}}\rangle$ involves contending with two dynamical processes of the system. In the superfluid and intermediate regimes ($\tau > \tau_1$), the hopping terms of the Hamiltonian (Eq. (2)) proportional to κ'' allow the quanta to redistribute into a site-localized superposition as τ is tuned. Adiabaticity with respect to κ'' must therefore be maintained while $\chi \leq \frac{4\kappa''_{max}}{n-1}$. From Fig. 7 of [54] we approximate the adiabatic condition for changing χ as $\frac{d\chi}{dt} \lesssim \frac{\kappa''_{max}}{10\tau_2(n-1)}$, which implies $\Delta t_1 \gtrsim 0.013\tau_2 \mu s$ for all $n > 5$, where Δt_1 is the time taken to adiabatically tune χ within the regime $\tau > \tau_1$. After the adiabatic tuning, χ can be non-adiabatically increased to χ_{max} . By increasing χ while κ'' is maximal, Δt_1 is minimized and therefore the effect of the transmon's minimal dephasing time in the vicinity of the flux "sweet spot" can be minimized. On the other hand, as discussed in [53], because perfect degeneracy of the lattice sites is not experimentally feasible there will be non-uniformity of the lattice population induced in the site basis at a rate $\Delta\epsilon/\hbar$, where $\Delta\epsilon$ is the difference between on-site energies. This is relevant in the intermediate and Schrödinger cat regimes ($\tau_2 > \tau$). If the intermediate regime is traversed on a time scale comparable to or longer than $\hbar/\Delta\epsilon$, the system will have time to transition to the global ground state of complete localization in the lowest energy site. We therefore require $\Delta t_{int} \ll \hbar/\Delta\epsilon$, where Δt_{int} is the time it takes to traverse the intermediate regime, so that the spatially uniform distribution of the quanta from the superfluid regime is maintained and the system ends up in a superposition of localization on each site. For the conservative estimate of $\Delta t_{int} \approx \Delta t_1$, this implies $\Delta\epsilon/\hbar \lesssim 2\pi \times 1.22/\tau_2$ MHz, which can be satisfied for moderate lattice sizes ($2 \leq M \leq 20$) as reference [73] demonstrates fabrication capability for GHz frequency CPW resonators with variations $\Delta\omega_c \approx 2\pi \times 1$ MHz, while contributions to

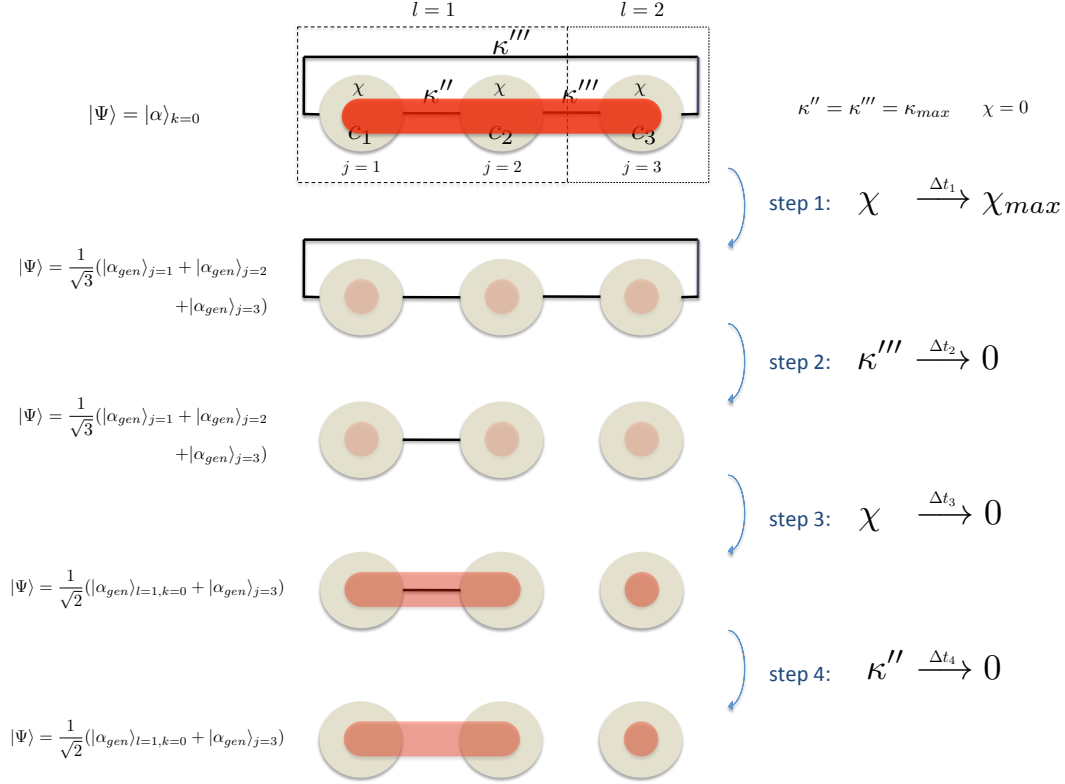


FIG. 2: Steps one, two, three, and four of the state preparation protocol illustrated for the case of a total of three sites in two blocks. Beige circles denote microwave CPW oscillator modes (c_j) with negative Kerr nonlinearities of strength χ . Solid black lines denote tunable intra-block (κ'') and inter-block (κ''') couplings. The coherent state indicated in red shading can be site-localized (circle) or distributed over adjacent sites (oblong). Darker shading intensity reflects higher occupation probability. An initial coherent state is created in the lowest energy normal mode of the lattice, then converted into a site-localized superposition $|\Psi_{\alpha_{gen}}\rangle$ by adiabatically increasing χ in step one. Due to the presence of the Kerr medium, the initial coherent state $|\alpha\rangle$ acquires a time-dependent shearing of its Wigner function and is therefore labeled as a generalized coherent state $|\alpha_{gen}\rangle$. In step two the blocks are decoupled by tuning κ''' to zero. In step three χ is adiabatically tuned back to zero to convert the state into the block-localized superposition $|\Psi_{\alpha_{gen}}^{(block)}\rangle$. In step four the sites within each block are decoupled and $|\Psi_{\alpha_{gen}}^{(block)}\rangle$ is then ready to be transferred to the mechanical modes b_j via state-swapping with modes a_j . The Wigner function shearing of $|\alpha_{gen}\rangle$ ceases at the end of step three when $\chi = 0$, and with appropriate timing the final state of each block corresponds to a superposition of the vacuum state $|0\rangle$ and either a squeezed coherent state $|\alpha_{sq}\rangle$ or a squeezed Schrödinger cat state $\frac{1}{\sqrt{2}}(e^{-i\pi/4}|i\alpha_{sq}\rangle_j + e^{i\pi/4}|-i\alpha_{sq}\rangle_j)$.

$\Delta\epsilon$ from intersite variations in χ_j can be minimized through experimental calibration of the control signals to keep the χ_j nearly equal during step one of the state preparation protocol. Once the superposition is achieved, intersite oscillations due to finite $\Delta\epsilon$ do not destroy the superposition.

Note that starting with an initial Fock state (with $N > 1$) instead of an initial coherent state would yield a W state. Our proposed scheme can therefore be an alternative to the one experimentally demonstrated by Wang et al. in [50], but with the added advantage of N being constrained by the number of sites M rather than qubit T_2 times: if each site is tunably coupled to a qubit, then M quanta can be simultaneously loaded (one in each mode c_j via the scheme demonstrated in [72]) while $\kappa'' = 0$, after which κ'' can be adiabatically tuned to κ_{max} to prepare the fixed number superfluid state as the initial state of step one.

After the first step, the state of the lattice is approximately $|\Psi_{\alpha_{gen}}\rangle$ (assuming $|\alpha|^2 \geq 14$). In the second step, $\kappa'''/2\pi$ is non-adiabatically tuned ($\Delta t_2 \approx 2$ ns) to 0.1 MHz to decouple the blocks, while leaving $\kappa'' = \kappa_{max}$. Because the state is in the Schrödinger cat regime, this does not alter the state.

The third step of the protocol expands the site-localized $|\alpha_{gen}\rangle$ of $|\Psi_{\alpha_{gen}}\rangle$ to the block-localized $|\alpha_{gen}\rangle$ of $|\Psi_{\alpha_{gen}}^{(block)}\rangle$. χ is tuned back to 0 (adiabatically for $\tau > 0.25$) so that the site-localized $|\alpha_{gen}\rangle$ become block-localized superfluid $|\alpha_{gen}\rangle$ and the state of the c_j lattice is $|\Psi_{\alpha_{gen}}^{(block)}\rangle$. From the discussion of the first step we know that this must be done on a timescale $\Delta t_3 \gtrsim \Delta t_1$ to maintain adiabaticity. Further, as discussed toward the end of section I., if α is sufficiently large the timing may be chosen such that $|\alpha_{gen}\rangle \approx |\alpha_{sq}\rangle$ or $|\alpha_{gen}\rangle \approx \frac{1}{\sqrt{2}}(e^{-i\pi/4}|\alpha_{sq}\rangle + e^{i\pi/4}|-i\alpha_{sq}\rangle)$. If there is only one block for the whole lattice, the latter case results in the squeezed GHZ-ECS.

In the fourth step, the intra-block couplings $\kappa''/2\pi$ are rapidly tuned ($\Delta t_4 \sim 2$ ns) to 0.1 MHz so that all the c_j modes are decoupled. This may alter the population distribution somewhat within each block due to imperfect diabaticity, but the superfluid nature (inter-site phase coherence) of the blocks is preserved as there is no onsite interaction.

In the final step, state transfer from c_j to a_j ($\Delta t_{5a} \approx 0.01$ μ s) then a_j to b_j ($\Delta t_{5b} \approx 0.1$ μ s) is done by pulsing κ' and g , respectively. Although the mechanical modes (b_j) at cryogenic temperatures will have significant thermal occupation, the experiment of [46] demonstrated that the state swap effectively cools the mechanical mode (b_j) by transferring the thermal quanta to the LC mode (a_j) so that the state of the mechanical mode (b_j) immediately

after the swap contains the desired state plus only about one thermal quantum. The end result is a purely mechanical Schrödinger cat state with a superposition of a generalized coherent state localized completely within blocks of physically adjacent but uncoupled micromechanical oscillators. For blocks with more than one oscillator, there is phase coherence between the oscillators of the block and the state of the block may be considered in this respect as a micromechanical superfluid. We note that the conversion from microwave to micromechanical can also be site-specific instead of lattice-wide, resulting in an entangled microwave-micromechanical state.

We can estimate the quantum coherence of the W-ECS after it is prepared and transferred to the mechanical modes. Using the formula $\frac{1}{T_{0n}} = \frac{n}{T_1} + \frac{n^2}{T_\phi}$ (see [74]), an average $T_1 \approx 2 \mu s$, and an average dephasing time of $T_\phi \approx 100 \mu s$ over the relevant flux range, we estimate the average decoherence over steps one, two, three, and four for a coherent superposition $|n\rangle|0\rangle + |0\rangle|n\rangle$ across two of the c_j modes to be $D_{1,2,3,4}(n) = e^{-(\Delta t_1 + \Delta t_2 + \Delta t_3 + \Delta t_4)(n/(2 \times 10^{-6}) + n^2/(100 \times 10^{-6}))}$. The decoherence $D_{5a}(n) = e^{-\Delta t_{5a}/T_{0n}}$ over Δt_{5a} will entail an average of the decay rates of the CPW and the LC oscillator (we assume dephasing to be negligible for both modes when $\chi = 0$): $T_{0n} = 2 \times 10^{-6}/n(\gamma_c + \gamma_a)$ $s = 3.42/n \mu s$. The decoherence $D_{5b}(n) = e^{-\Delta t_{5b}/T_{0n}}$ over Δt_{5b} will entail an average of the decay rates of the LC oscillator and the mechanical mode (we assume dephasing to be negligible for these modes): $T_{0n} = 2 \times 10^{-6}/n(n_{env}\gamma_b + \gamma_a)$ $s = 7.67/n \mu s$, where $n_{env} = 50$ is due to the mechanical mode thermal environment at 25 mK [46]. In Fig. (3) we plot the total remaining quantum coherence of an initial bipartite W-ECS with amplitude α after all of the preparation stages under the approximation that the time in step one during which $\tau > 0.25$ is negligible: $\sum_{n=0}^{1000} |\langle n|\alpha \rangle|^2 D_{1,2,3,4}(n) D_{5a}(n) D_{5b}(n)$ vs. $|\alpha|$. The plot indicates that our proposed system and protocol can achieve at each site a purely mechanical cat state with greater than fifty percent initial quantum coherence and an average centre of mass spatial separation several times the mechanical zero point motion.

III. NUMERICAL SIMULATION

We provide a proof of principle demonstration of our proposal through numerical simulations of steps one, two, and three of our state preparation protocol with realistic parameters as given in section I. A two site lattice ($M = 2, \tau_2 = 0.25$) is considered with an initial

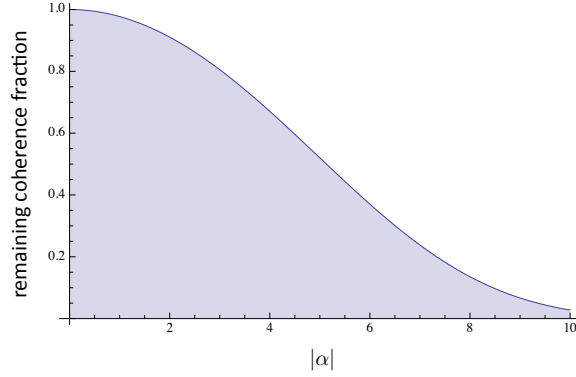


FIG. 3: Remaining fraction of quantum coherence as a function of coherent state amplitude $|\alpha|$ of initial bipartite W-ECS after transfer to mechanical modes. The calculation is done under the approximation that the time spent in the superfluid regime ($\tau > 0.25$) is negligible.

coherent state of amplitude $|\alpha|^2 = 20$ in the lowest energy normal mode. As steps one, two, and three occur on a timescale of $\Delta t_1 + \Delta t_2 + \Delta t_3 \approx 10$ ns, we may obtain a qualitatively valid result by neglecting damping. The Hilbert space at each site is truncated at $n_{max} = 27$. The timing of each step is chosen to respect the minimum tuning times of each device, to satisfy the adiabaticity constraint, and to end step three near a fidelity oscillation peak so that the state of the system settles on a squeezed W-ECS.

Fig. (4) shows the time-evolution of the fidelity of the system state with an ideal W-ECS state ($|\langle \Psi | \Psi_{W-ECS} \rangle|$) through steps one and two and then a brief additional period of no tuning. χ is tuned from zero to χ_{max} in 5 ns, after which κ'' is tuned to zero in 2 ns. The subsequent no tuning period of 0.5 ns is for timing purposes so that the following step ends near a fidelity oscillation peak. Fig. (5) shows the evolution of the fidelity through step three, where χ is tuned back to zero in 5 ns. The oscillations of the fidelity are indicative of the cyclic phase shearing of the site-localized coherent state in phase space due to the nonlinearity in each site of the lattice. The oscillations increase (decrease) in frequency as χ is increased (decreased). The imperfect maximum fidelity is due to the fact that the coherent state is actually squeezed due to the phase shearing that occurs in step one while $\tau > 0.25$, as discussed at the end of section I. This is revealed in Fig. (6), where we plot at the final fidelity peak of step three the Wigner function of the density matrix for the first site obtained by tracing the system density matrix over the second site. The single

particle correlator $|\langle c_1^\dagger c_2 \rangle|$ between sites one and two is plotted in Fig. (7) over the whole simulation time. The steady decrease of $|\langle c_1^\dagger c_2 \rangle|$ indicates increasing site-localization of the initial coherent state, while the intermittent oscillation pulses are not understood. The perfect ECS has complete site-localization and a single particle correlator value of zero.

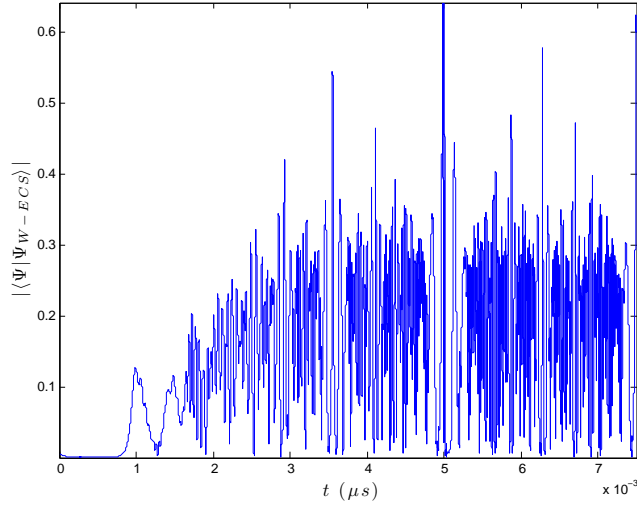


FIG. 4: Fidelity of the system state with an ideal W-ECS state over a simulation of steps one and two of the state preparation protocol for an initial coherent state of amplitude $|\alpha|^2 = 20$ in the lowest energy normal mode of a two site chain of CPWs. A $0.5 \mu s$ period of unitary evolution is included after step two for protocol timing purposes.

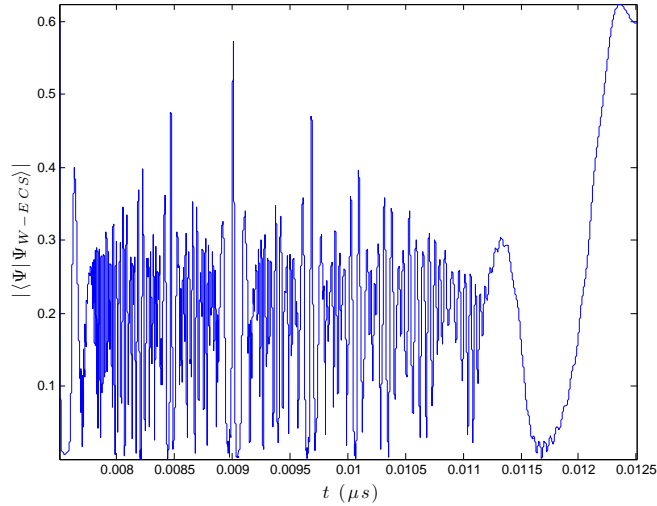


FIG. 5: Fidelity of the system state with an ideal W-ECS state over a simulation of step three of the state preparation protocol for an initial coherent state of amplitude $|\alpha|^2 = 20$ in the lowest energy normal mode of a two site chain of CPWs.

IV. DETECTION

Detection of the W-ECS/W-ESCS/GHZ-ECS may be done by swapping it into the a_j modes and using controllably coupled superconducting qubits (as in the case of [75]) for bipartite Wigner tomography [50] between different pairs of sites. Alternatively, the scheme of Tuferelli et al. [76] may be used wherein the initial state of a linear oscillator network is reconstructed through readout of a single qubit attached to a single oscillator in the network. After creation of the mechanical/microwave W-ECS/W-ESCS/GHZ-ECS in our system, all

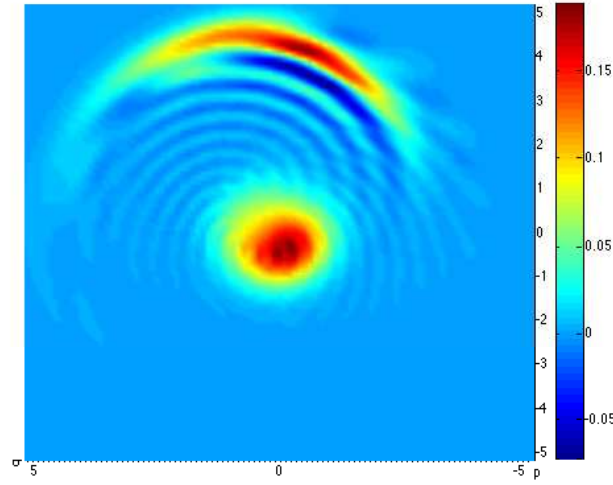


FIG. 6: The Wigner function for the first site at the fidelity peak near the end of step three reveals a coherent superposition of a vacuum state and a quadrature squeezed coherent state of amplitude $|\alpha| = \sqrt{20}$.

couplings κ' , κ'' , and g could be turned on while leaving $\chi = 0$ to make the network linear. A single qubit tunably coupled to any microwave mode in our system could then be used to reconstruct the initial mechanical/microwave W-ECS/W-ESCS/GHZ-ECS of the system. One caveat of this approach is that it requires Markovian master equation modelling of the dissipative environment for all of the oscillators of the network. Because the correct such model for the mechanical dissipation is unknown, the bipartite Wigner tomography method may need to be used to first verify which dissipative model to use before applying the method

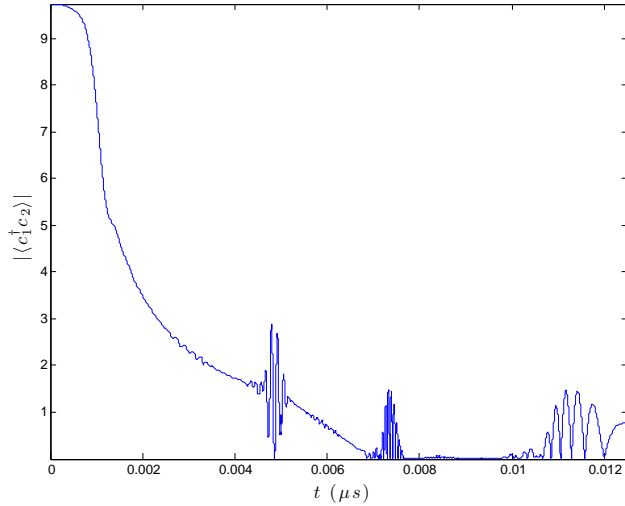


FIG. 7: $|\langle c_1^\dagger c_2 \rangle|$ over the whole simulation period. The ideal ECS should have a value of zero, indicating complete site-localization.

of Tufarelli to read out the entire network.

V. CONCLUSION AND OUTLOOK

We have proposed a way to use existing superconducting circuit technology to experimentally simulate the dynamical manipulation of a many-body Hamiltonian for the purpose of producing a multipartite squeezed ECS of the W- or GHZ-type in the microwave domain. Our proposal presents a new paradigm for deterministic ECS generation that is highly relevant in the face of on-going developments in superconducting circuit-based fundamental

quantum tests, quantum simulation, and quantum information processing. With appropriate timing of our protocol, the squeezed ECS may take the form of a non-locally superposed squeezed coherent state or a non-locally superposed squeezed cat state. We have further shown how to combine existing electromechanical technology with the proposed superconducting circuit to convert the multipartite photonic quantum state into a purely mechanical one, thereby enabling the simultaneous observation of three thus far unobserved quantum phenomena in mechanical systems: multipartite non-gaussian entanglement, quadrature squeezing below the standard quantum limit, and Schrödinger cats. This new approach to the preparation of entangled mechanical oscillators is one that is more readily scalable to many oscillators and thereby more promising for applications. Also, because our protocol accesses large ($|\alpha|^2 > 10$) squeezed coherent state mechanical Schrödinger cats, it may prove useful for fundamental tests in the mechanical realm. At a more general level, our proposal suggests the use of quantum phase transitions as a resource for fundamental and applied studies in engineered quantum systems.

Acknowledgments

We acknowledge the support of the Australian Research Council Centre of Excellence for Engineered Quantum Systems (grant number CE110001013). AAG acknowledges support from the UQRS/UQIRTA scholarships and helpful discussions with Jerome Bourassa.

Appendix

Consider the Hamiltonian given in Eq.(2) for the case of two sites,

$$\frac{H}{\hbar} = -\frac{\chi_1(t)}{2}c_1^\dagger c_1(c_1^\dagger c_1 - 1) - \frac{\chi_2(t)}{2}c_2^\dagger c_2(c_2^\dagger c_2 - 1) - \kappa''(t)(c_1^\dagger c_2 + c_1 c_2^\dagger), \quad (3)$$

with the explicit assumption that each of the quartic non-linear terms and the quadratic coupling term may be subject to independent control.

We begin by assuming that the Kerr nonlinearity is set to zero. Then both normal modes, $A_1 = (a_1 + a_2)/\sqrt{2}$, $A_2 = (a_1 - a_2)/\sqrt{2}$, of the coupled cavity system can each be coherently driven to a steady-state coherent state. The state of the local modes is likewise a product coherent state, and by a suitable choice of the normal mode driving fields it

becomes $|\alpha\rangle_{a_1} | -\alpha\rangle_{a_2}$. In the first step we set κ'' to zero, to decouple the cavities, and the Kerr nonlinear term for cavity a_1 is to a non-zero value for a fixed time T_1 such that $\chi T_1 = \pi$. The Kerr nonlinearity for mode a_2 remains set at zero. This transforms the local modes as

$$|\alpha\rangle_{a_1} | -\alpha\rangle_{a_2} \rightarrow \frac{1}{\sqrt{2}} (e^{-i\pi/4} |i\alpha\rangle_{a_1} + e^{i\pi/4} | -i\alpha\rangle_{a_1}) | -\alpha\rangle_{a_2} \quad (4)$$

In the next step we turn on the coupling between the cavities for a fixed amount of time T_2 so that $\kappa'' T_2 = \pi/4$, the resulting state is

$$e^{-i\pi/4} |i\sqrt{2}\alpha\rangle_{a_1} |0\rangle_{a_2} + e^{i\pi/4} |0\rangle_{a_1} | -\sqrt{2}\alpha\rangle_{a_2} \quad (5)$$

While this is not precisely a W-ECS it is a non-classical entangled cat state. Using suitable phase rotations and displacements however it can easily be transformed into a W-ECS state.

-
- [1] M. Aspelmeyer, P. Meystre, K. Schwab, *Physics Today* 65 (7), 29 (2012).
 - [2] G. J. Milburn and M. J. Woolley, *Acta Physica Slovaca* 61, no. 5 (2012).
 - [3] A. D. O'Connell et al., *Nature* 464, 697 (2010).
 - [4] L. Tian, *Phys. Rev. B* 72, 195411 (2005).
 - [5] S. Mancini, V. Giovannetti, D. Vitali and P. Tombesi, *Phys. Rev. Lett.* 88 120401 (2002).
 - [6] M. J. Woolley, G. J. Milburn, C. M. Caves, *New J. Phys.* 10 12501 (2008).
 - [7] E. Gavartin, P. Verlot, T. J. Kippenberg, *Nature Nanotech.* 7, 509 (2012).
 - [8] F. Massel, T. T. Heikkilä, J.-M. Pirkkalainen, S. U. Cho, H. Saloniemi, P. J. Hakonen, M. A. Sillanpää, *Nature* 480, 351 (2011).
 - [9] M. Bagheri, M. Poot, M. Li, W. P. H. Pernice, H. X. Tang, *Nature Nanotech.* 6, 726732 (2011).
 - [10] K. Stannigel, P. Rabl, A. S. Sørensen, P. Zoller, and M. D. Lukin, *Phys. Rev. Lett.* 105, 220501 (2010).
 - [11] K. Stannigel, P. Rabl, A. S. Sørensen, M. D. Lukin, and P. Zoller, *Phys. Rev. A* 84, 042341 (2011).
 - [12] A. V. Tsukanov, *Russian Microelectronics* 40, 254 (2011).
 - [13] I. Pikovski, M. R. Vanner, M. Aspelmeyer, M. S. Kim and C. Brukner, *Nat Phys* 8, 393397 (2012).

- [14] O. Romero-Isart, A. C. Pflanzer, F. Blaser, R. Kaltenbaek, N. Kiesel, M. Aspelmeyer, J. I. Cirac, Phys. Rev. Lett. 107, 020405 (2011).
- [15] A. Bassi et al., arXiv:1204.4325.
- [16] B. Pepper et al., arXiv:1207.1946.
- [17] B. C. Sanders, Phys. Rev. A 45, 6811-6815 (1992); B. C. Sanders, Phys. Rev. A 46, 2966 (1992).
- [18] B. C. Sanders, J. Phys. A: Math. Theor. 45, 244002 (2012).
- [19] The transition that we use can not strictly be termed a *quantum phase transition* as the thermodynamic limit for the Hamiltonian we employ is ill-defined (see [56]).
- [20] A. N. Cleland and M. L. Roukes, in Proceedings ICPS-24, edited by D. Gershoni (World Scientific, Singapore, 1999).
- [21] S. Bose, K. Jacobs and P. L. Knight, Phys. Rev. A 59, 3204 (1999).
- [22] M. P. Blencowe and M. L. Wybourne, Physica B 280,555 (2000).
- [23] S.M. Carr, W.E. Lawrence, and M.N. Wybourne, Phys. Rev. B 64, 220101 (2001).
- [24] A. D. Armour, M. P. Blencowe and K. C. Schwab, Phys. Rev. Lett. 88, 148301 (2002).
- [25] W. Marshall et al., Phys. Rev. Lett. 91, 130401 (2003).
- [26] M. Blencowe, Physics Reports 395, 159 (2004).
- [27] K. C. Schwab and M. L. Roukes, Phys. Today 58, 36 (2005).
- [28] A. J. Leggett, Contemporary Physics, 25:6, 583 (1984); A. J. Leggett, J. Phys.: Condens. Matter 14, R415 (2002).
- [29] L. Tian and S. M. Carr, Phys. Rev. B 74, 125314 (2006).
- [30] W. J. Munro, K. Nemoto, G. J. Milburn, and S. L. Braunstein, Phys. Rev. A 66, 023819 (2002).
- [31] V. B. Braginsky and F. Ya. Khalili, *Quantum Measurement*, Cambridge University Press, Cambridge, 1992; M. F. Bocko and R. Onofrio, Rev. Mod. Phys. 68, 755 (1996).
- [32] W. H. Zurek, Rev. Mod. Phys., 75, 715 (2003).
- [33] M. Schlosshauer, A. P. Hines, G. J. Milburn, Phys. Rev. A 77, 022111 (2008).
- [34] L. G. Remus, M. P. Blencowe, Y. Tanaka, Phys. Rev. B 80, 174103 (2009).
- [35] S. Bose and G. S. Agarwal, New Journal of Physics 8, 34 (2006).
- [36] L. Tian and P. Zoller, Phys. Rev. Lett. 93, 266403 (2004).
- [37] W. J. Munro, G. J. Milburn, and B. C. Sanders, Phys. Rev. A 62, 052108 (2000); K. Park

- and H. Jeong, Phys. Rev. A 82, 062325 (2010).
- [38] A. Ourjoumtsev, Nature Physics 5, 189 (2009).
 - [39] R. Chaves and L. Davidovich, Phys. Rev. A 82, 052308 (2010); A. Montakhab and A. Asadian, Phys. Rev. A 77, 062322 (2008); A. R. R. Carvalho, F. Mintert, and A. Buchleitner, Phys. Rev. Lett. 93, 230501 (2004).
 - [40] A. A. Houck, H. E. Tureci, and J. Koch, Nature Physics 8, 292 (2012).
 - [41] This is in contrast to the scheme of Wang and Sanders [42], which considers how to generate an ECS amongst the different normal modes of a single chain of coupled ions.
 - [42] X. Wang and B. C. Sanders, Phys. Rev. A 65, 012303 (2001).
 - [43] J. D. Teufel et al., Nature **471**, 204 (2011).
 - [44] J. D. Teufel et al., Nature **475**, 359 (2011).
 - [45] J. Bourassa, F. Beaudoin, J. M. Gambetta, and A. Blais, Phys. Rev. A 86, 013814 (2012).
 - [46] T. A. Palomaki et al., arXiv:1206.5562.
 - [47] R. C. Bialczak et. al, Phys. Rev. Lett. 106, 060501 (2011).
 - [48] Y. Yin et al., arXiv:1208.2950.
 - [49] J. D. Teufel, private communication.
 - [50] H. Wang et al., Phys. Rev. Lett. 106, 060401 (2011).
 - [51] A. A. Houck et al., Quantum Inf. Process. 8, 105 (2005).
 - [52] J. Bourassa, private communication.
 - [53] M. W. Jack and M. Yamashita, Phys. Rev. A 71, 023610 (2005).
 - [54] P. Buonsante et al., Phys. Rev. A 72, 043620 (2005).
 - [55] P. Buonsante et al., J. Phys. B (2006).
 - [56] N. Oelkers and J. Links, Phys. Rev. B 75, 115119 (2007).
 - [57] P. Buonsante et al., Phys. Rev. A 82, 043615 (2010).
 - [58] J. I. Cirac, Phys. Rev. A 77, 033403 (2008).
 - [59] G. Mazzarella, L. Salasnich, A. Parola, and F. Toigo, Phys. Rev. A 83, 053607 (2011).
 - [60] J. I. Cirac, M. Lewenstein, K. Molmer, and P. Zoller, Phys. Rev. A 57, 1208 (1998).
 - [61] M. J. Steel and M. J. Collett, Phys. Rev. A 57, 2920 (1998).
 - [62] P. Zin, Euro. Phys. Lett. 83, 64007 (2008).
 - [63] M. Lieb and M. J. Hartmann, New J. Phys. 12, 093031 (2010).
 - [64] M. J. Hartmann, F. G. S. L. Brandao, and M. B. Plenio, Nat. Phys. 2, 849 (2006).

- [65] S. Lloyd and S. L. Braunstein, Phys. Rev. Lett. 82, 1784 (1999).
- [66] D. F. Walls and G. J. Milburn, *Quantum Optics* (1994).
- [67] G. Kirchmair et al., arXiv:1211:2228.
- [68] N. B. An, Phys. Rev. A 69, 022315 (2004).
- [69] H. Jeong and N. B. An, Phys. Rev. A 74, 022104 (2006).
- [70] M.-F. Chen and S.-S. Ma, Acta Photon. Sin. 36950 (2007).
- [71] Y. Guo and L. M. Kuang, J. Phys. B: At. Mol. Opt. Phys. 40, 3309 (2007).
- [72] M. Hofheinz et al., Nature **454**, 310 (2008).
- [73] D. Underwood et al., Phys. Rev. A 86, 023837 (2012).
- [74] X.-Y. Chen and L.-Z. Jiang, J. Phys. B: At. Mol. Opt. Phys. 40, 2799 (2007).
- [75] M. S. Allman, F. Altomare, J. D. Whittaker, K. Cicak, D. Li, A. Sirois, J. Strong, J. D. Teufel, and R.W. Simmonds, Phys. Rev. Lett. 104, 177004 (2010).
- [76] T. Tufarelli et al., Phys. Rev. A 85, 032334 (2012).